VARIABLE RANGE-HOPPING CONDUCTIVITY IN $Cu_2ZnSiSe_4$

M. Guc

Institute of Applied Physics, Academy of Sciences of Moldova, Academiei str. 5, Chisinau, MD 2028 Republic of Moldova
E-mail: gmax@phys.asm.md

(Received 1 March 2013)

Abstract

Single crystals of p-$Cu_2ZnSiSe_4$ were grown by chemical vapour transport using iodine as a transported agent. The temperature dependence of the resistivity is investigated in a range of T ~ 10–300 K. The Mott variable-range hopping conductivity is observed at T ~ 70–210 K. Its detailed analysis has yielded the values of the microscopic parameters, including the relative acceptor concentration, the critical concentration of the metal-insulator transition, the relative localization radius, the width of the acceptor band, and the average density of the localized states.

1. Introduction

$Cu_2ZnSiSe_4$ belongs to the group of quaternary compounds with a wurtzstannite type structure [1-5]. These materials have attracted considerable interest because of there nonlinear optic [6, 7], thermoelectric [8], and optoelectronic [9] properties. Their possible application as wide band gap absorbers in solar cells is also discussed [10]. The orthorhombic crystal lattice of $Cu_2ZnSiSe_4$ is characterized by the space group P$mn2_1$. This structure possesses alternating cation layers of mixed Zn and Si atoms, which are separated by layers of Cu atoms. Each selenium atom has four nearest neighbouring metal atoms localized at the corners of the surrounding tetrahedron, two copper, one zinc, and one silicon atom [4]. On the other hand, a new wurtzite-kesterite structure, which is derived from the wurtzstannite one by mixing of Cu and Zn atoms, has been proposed [11]. The space group of this structure is Pc and the lattice is pseudo-orthorhombic, which allows the same configuration of metal atoms around Se as in the wurtzstannite structure [4]. The calculated total energy for wurtzite-kesterite structure slightly exceeds that of the kesterite structure and is much lower than the respective energy of the wurtzstannite structure [11]. The calculated enthalpy of formation is also lower for the kesterite structure than for the wurtzstannite one [10]. Nevertheless, information about growth of $Cu_2ZnSiSe_4$ with a kesterite or wurtzite-kesterite structure is lacking. The single crystalline X-ray diffraction (XRD) microanalysis was performed in [12] and the orthorhombic wurtz-stannite type structure was confirmed. The effective electron and hole masses of the kesterite and the stannite modifications of $Cu_2ZnSiSe_4$ were evaluated with the first-principle calculations [13].

In addition to structural and theoretical investigations, the optical band gap was studied [3, 4, 14, 15]. However, the details of the energy spectrum near the band gap are not completely clear. So, the energies of direct transitions of about 2.33–2.35 eV at room temperature were obtained in [3, 15]. The room temperature energies of the indirect transitions were estimated to lie approximately between 2.08–2.20 eV in [4, 14]. The splitting of the valence band was also discussed [14, 15]. The IR absorption bands [4], the Knoop hardness [4], the vibrational [5, 16] and irradiative [16] properties of $Cu_2ZnSiSe_4$ have been studied. Investigations of transport

properties have yielded values of the resistivity, ρ (300 K) ≈ 2×10^3 Ω cm [3] and 3×10^4 Ω cm [4]. However, information about the low-temperature transport properties of $Cu_2ZnSiSe_4$ is lacking.
Here we investigate the temperature dependence of the resistivity of $Cu_2ZnSiSe_4$ single crystals in a range of T ~ 10–300 K and focus attention on the Mott variable-range hopping (VRH) conduction. Analysis of the Mott VRH conductivity makes it possible to obtain interesting information on the microscopic properties of charge carriers in this material.

2. Experimental

Single crystals of $Cu_2ZnSiSe_4$ were grown by chemical vapour transport from stoichiometric amounts of the elements with 5 mg iodine per cm^3 as the transport agent. Optimum crystal growth was achieved with the charge zone maintained at 850°C and the growth zone at 800°C. The transport process was carried out for a period of 14 days. Single crystals of $Cu_2ZnSiSe_4$ were formed with a thin orange blade shape given by an area of up to 20×1.0 mm^2 and by a thickness of 100 μm. The chemical composition of the obtained crystals was investigated by An INCA Energy 200 EDX system (OXFORD Instruments) attached to a TESCAN VEGA 5130 MM Scanning Electron Microscope (see Table I).

Table 1. Chemical compositions of the investigated $Cu_2ZnSiSe_4$ single crystals

Sample	Cu (at. %)	Zn (at. %)	Si (at. %)	Se (at. %)	Formula
SiSe_1	23.8	12.0	14.2	50.0	$Cu_{1.90}Zn_{0.96}Si_{1.14}Se_{4.00}$
SiSe_2	25.6	12.8	13.0	48.6	$Cu_{2.05}Zn_{1.02}Si_{1.04}Se_{3.89}$
SiSe_3	23.3	11.7	14.3	50.7	$Cu_{1.86}Zn_{0.94}Si_{1.14}Se_{4.06}$
SiSe_4	25.5	12.4	13.5	48.6	$Cu_{2.04}Zn_{0.99}Si_{1.08}Se_{3.89}$
SiSe_5	24.0	12.0	13.8	50.2	$Cu_{1.92}Zn_{0.96}Si_{1.10}Se_{4.02}$

Resistivity ρ (T) was measured with the van der Pauw method at temperatures T between 10–300 K. The contacts were made by a mixture of In and Ga with a silver paste as fixing compound. To avoid the uncontrolled heating of the sample during the measurements, the applied current was kept less than 100 μA. The hot probe method showed the p-type conductivity of the investigated $Cu_2ZnSiSe_4$ crystals. The rotating orientation X-ray diffraction method revealed that the long-edge fringe of the crystal platelets was parallel to the ***c*** axis, and the resistivity was measured along this axis. The obtained dependences of ρ (T) are shown in Fig. 1.

3. Results and Discussion

3.1. The interval of the Mott VRH conduction and macroscopic parameters

The interval of the Mott VRH conductivity mechanism can be identified with two methods. The first one is based on the equation representing the theoretical dependence of the resistivity [17, 18]:

$$\rho(T) = AT^{1/4}\exp\left[\left(\frac{T_0}{T}\right)^{1/4}\right], \quad (1)$$

where A is the prefactor constant (independent of T) and T_0 is the VRH characteristic temperature. It is evident from Eq. (1), that the plots of ln ($\rho/T^{1/4}$) vs. $T^{-1/4}$ should be linear. Figure 2 presents the plots above fitted with a linear function. The respective macroscopic parameters, including the temperature interval of the linearity of the plots in Fig. 2, the characteristic temperatures, and the prefactor constants, are collected in Table II for all the investigated samples.

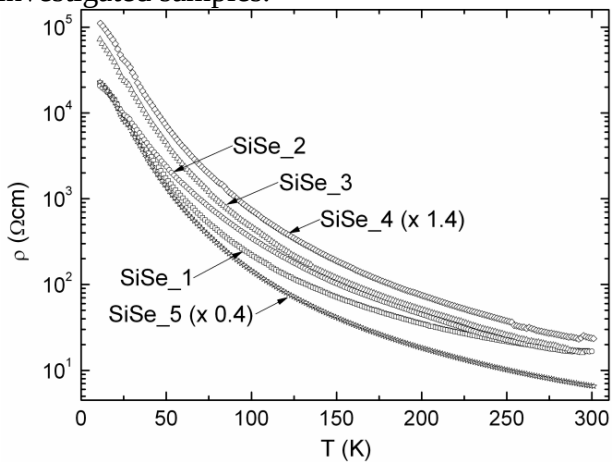

Fig. 1. Temperature dependence of the resistivity of $Cu_2ZnSiSe_4$ single crystals.

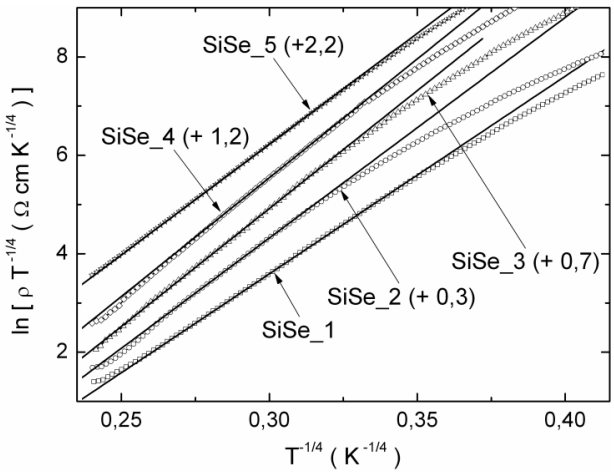

Fig. 2. Plots of ln ($\rho T^{1/4}$) vs. $T^{-1/4}$ for investigated samples of $Cu_2ZnSiSe_4$. For convenience, some of the plots are shifted along the vertical axis by the values given in parenthesis. The straight lines are linear fits.

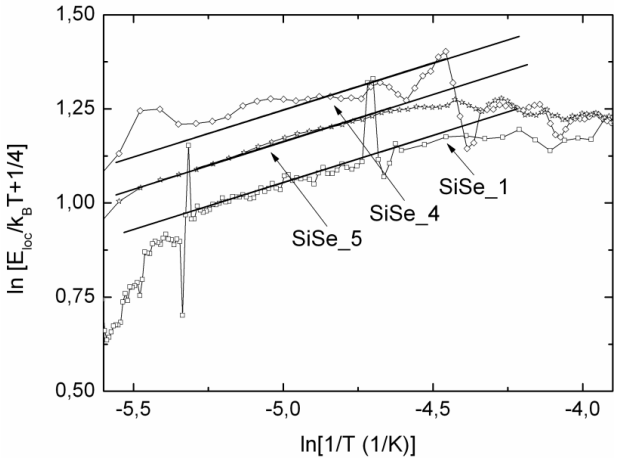

Fig. 3. Plots of ln[$E_{loc}/(k_BT)$ + 1/4] vs. ln(1/T) for some of the investigated samples. The straight lines correspond to the constant slope of 1/4.

The second method of identification of the Mott VRH conductivity mechanism is based on the analysis of the local activation energy [18]:

$$E_{loc}(T) = \frac{d[\ln \rho(T)]}{d[(k_B T)^{-1}]}. \quad (2)$$

Combining Eqs. (1) and (2), the following expression can be obtained:

$$\ln(E_{loc} / k_B T + 1/4) = \ln(1/4) + (1/4)\ln(T_0) + (1/4)\ln(1/T). \quad (3)$$

The plots of $\ln(E_{loc}/k_BT + 1/4)$ vs. $\ln(1/T)$ together with linear fits with a constant slope of 1/4 are presented in Fig. 3. The respective macroscopic parameters of the Mott VRH conductivity obtained with the second method are also collected in Table II.

The two above described methods yield quite similar values of all the macroscopic parameters (see Table II).

Table 2. Prefactor constant A and characteristic temperature T_0 obtained in the Mott VRH interval ΔT_M with two different methods

Sample	Linearization of the resistivity			Analysis of the local activation energy	
	A ($10^{-5}\Omega$ cm $K^{-1/4}$)	ΔT_M (K)	T_0 (10^6 K)	ΔT_M (K)	T_0 (10^6 K)
SiSe_1	21.2	70 – 210	2.6	85 – 200	2.6
SiSe_2	8.1	115 – 200	4.0	120 – 200	4.1
SiSe_3	3.9	90 – 190	5.3	100 – 200	5.4
SiSe_4	13.1	80 – 185	5.4	85 – 210	5.6
SiSe_5	7.6	90 – 210	4.1	100 – 200	4.0

3.2. Microscopic parameters

The characteristic temperature of the Mott VRH conductivity depends on the density of localized states (DOS) $g(\mu)$ at the Fermi level μ and on the localization radius of the holes a [18] as follows:

$$T_0 = \frac{\beta}{k_B a^3 g(\mu)}. \quad (4)$$

Here $\beta \approx 21$ is a numerical constant, and the localization radius of the holes is given by the equation

$$a = a_0(1 - N / N_c)^{-\nu}, \quad (5)$$

where N is the acceptor concentration, N_c is the critical concentration of the metal-insulator transition (MIT), and $\nu \approx 1$ is the critical exponent of the correlation length [19]. The localization radius of the acceptor states far from the MIT $a_0 = \hbar(2mE_0)^{-1/2}$, almost coincides with the Bohr radius of a hydrogenic impurity $a_B = \hbar^2\kappa_0(me^2)^{-1}$. Here m is the hole effective mass, E_0 is the energy difference between the maximum of the DOS and the bottom of the valence band, and κ_0 is the dielectric permittivity far from the MIT. The parameters N_c and a_0 are interrelated with the Mott universal criterion [17]: $N_c^{1/3} a_0 \approx 0.25$.

According to [17-19], the localization radius of holes can be also presented as

$$a = a_B(1 - E_c / \mu)^{-\nu}. \quad (6)$$

Equation (6) describes the case of a symmetric Anderson-type acceptor band with semi-width W and mobility edges $-E_c$ and E_c [17], as it is shown in Fig. 4. In this model, the broadening of an isolated acceptor level with the energy E_0 is due to a microscopic disorder, whereas the band contains both the localized and delocalized states. The localized states are shaded in Fig. 4, and the activated behaviour of the conductivity takes place if μ lies in the shaded areas. The position of μ in the delocalized state interval leads to the metallic or activationless conductivity. Eventually, if μ crosses E_c or $-E_c$, the Anderson MIT takes place. The mobility edge satisfies the expression

$$E_c \approx W - \frac{V_0^2}{4(z-1)J}, \tag{7}$$

where $z \approx 6$ is the number of the nearest neighbors in the acceptor system, V_0 represents a scale of scattering of the hole energy due to the cation disorder, and $J = J_0 \exp(-R/a_B)$ is the overlap integral [17]. Here $R \approx (4\pi N/3)^{-1/3}$ is the half of the mean distance between the acceptors, and the prefactor J_0 satisfies the equation [17]:

$$J_0 \approx \frac{e^2}{\kappa_0 a_B}\left[\frac{3}{2}\left(1+\frac{R}{a_B}\right)+\frac{1}{6}\left(\frac{R}{a_B}\right)^2\right]. \tag{8}$$

The semi-width W obeys the expression [17]:

$$W = 0.5 k_B (T_v^3 T_0)^{1/4}. \tag{9}$$

Here T_v is the high-temperature border of the Mott VRH conductivity, provided that μ lies close to W or $-W$. This takes place for $K << 1$ and $1 - K << 1$, respectively, where $K = N_D/N_A$ is the degree of the compensation and N_D is the donor concentration.

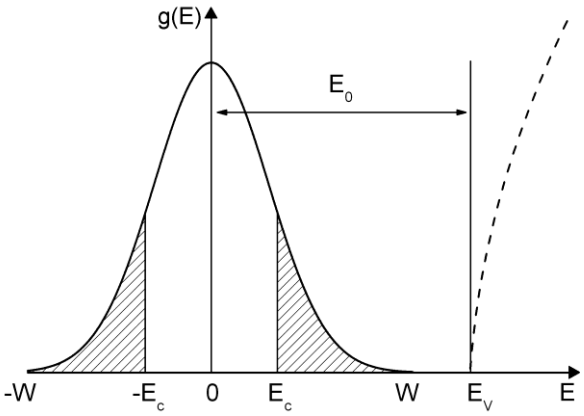

Fig. 4. DOS of the acceptor band (solid line) and of the valence band (dashed line) in the case of $E_0 > W$. The localized states of the acceptor band are hatched (schematically).

Combining Eqs. (4), (5), and (9), taking into account the universal Mott criterion for the MIT and approximating the DOS of the acceptor band with a rectangular shape, $g(\varepsilon) \approx g_{av} \equiv N/(2W) = g(\mu)$, as it has been previously used for a similar quaternary compound Cu_2ZnSnS_4 [20], the following expression can be obtained:

$$\left(\frac{T_0}{T_v}\right)^{1/4} \approx 4\beta^{1/3}\left(\frac{N_c}{N}\right)^{1/3}\left(1-\frac{N}{N_c}\right)^{\nu}. \quad (10)$$

At ν = 1 and with T_0 and T_v from Table II, the values a/a_0 and N/N_c are calculated and collected in Table III.

Equations (6)–(8) yield the ratio of a/a_B putting $V \approx 2W$, using the expression for a_B and the mean value of the hole effective mass $m \approx (m_\perp^2 m_\parallel)^{1/3}$ [18]. The latter has been calculated with the data from [13], and the value of $m = 0.38 \pm 0.04$ insignificantly varies for the kesterite and stannite modifications of $Cu_2ZnSiSe_4$. The next step of our analysis is to estimate the value of κ_0. For this purpose, we minimized the standard deviation $SD(a) = \left\{\frac{1}{5}\sum_{i=1}^{5}[(a/a_0)_i - (a/a_B)_i]^2\right\}^{1/2}$, where i is the sample number, taking into account that $a_0 \approx a_B$. According to Table III, there is good agreement between the values of a/a_0 and a/a_B, given by $SD(a) \approx 0.127$, at $\kappa_0 \approx 8.9$. Then the values of $a_0 \approx a_B \approx 12.4$ Å and $E_0 \approx 65$ meV are found with the expressions for the localization and the Bohr radii given above, and $N_c \approx 8.1\times10^{18}$ is obtained with the universal Mott criterion for the MIT. Table III also lists the values of E_c and g (μ) evaluated with Eqs. (7) and (4), respectively.

It follows from Table III that the value of W exceeds E_0, which contradicts to the model of DOS in Fig. 4. Therefore, the hole spectrum should be modified to that in Fig. 5. This modification does not have an effect on the microscopic values calculated above. However, the Fermi level can lie now only in the region of the localized states ($-W$, $-E_c$), which corresponds to strong degree of the compensation, $1 - K << 1$. This assumption should be verified by additional investigations, e. g. of the Hall effect and magnetoresistance. In addition, because in the calculations above we have used the rectangular shape of the DOS, which is rather crude, the obtained microscopic values can be considered rather as estimations.

Table 3. Values of N/N_c, a/a_0, a/a_B, W, E_c, and g_{av} in the investigated samples

Sample	N/N_c	a/a_0	a/a_B	W (meV)	E_c (meV)	g_{av} (10^{16} meV^{-1}cm^{-3})
SiSe_1	0.34	1.51	1.72	95	40	1.43
SiSe_2	0.29	1.41	1.41	102	29	1.14
SiSe_3	0.26	1.35	1.22	106	19	0.98
SiSe_4	0.25	1.34	1.21	106	18	0.97
SiSe_5	0.29	1.41	1.38	106	29	1.12

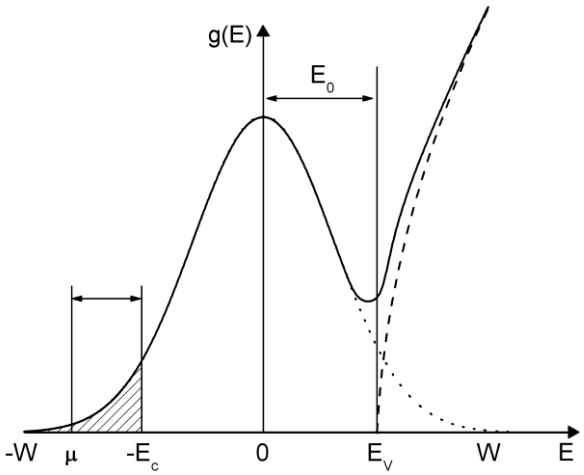

Fig. 5. Joint spectrum of the DOS near the edge of the valence band in the case of $E_0 < W$ (solid line). The localized states are hatched. The dashed and dotted lines represent the imaginative near-edge intervals of the valence and acceptor band, respectively, corresponding to the absence of their overlap (schematically).

5. Conclusions

The temperature dependence of the resistivity of $Cu_2ZnSiSe_4$ single crystals was investigated. The Mott type of the variable-range hopping conductivity was identified in the region of ~70–210 K for five samples. Analysis of the macroscopic parameters (A, T_v and T_0) has yielded a set of the microscopic parameters characterizing the hole concentration, the energy spectrum, and the localization radii of the holes $Cu_2ZnSiSe_4$. The DOS model was proposed, assuming a high lattice disorder and a high degree of compensation.

Acknowledgments. This work was supported by the IRSES PVICOKEST – 269167 projects. The author thanks Prof. E. Arushanov and Dr. K. G. Lisunov for the data analysis, Dr. Hab. V. Ursaki for the sample characterization, and Dr. S. Levcenco for the sample preparation and measurements.

References

[1] R. Nitsche, D.F. Sargent, and P. Wild, J. Cryst. Growth 1, 52–53 (1967).
[2] W. Schafer and R. Nitsche, Mater. Res. Bull. 9, 645–654 (1974).
[3] D.M. Schleich and A. Wold, Mat. Res. Bull. 12, 111-114 (1977).
[4] G-Q. Yao, H-S. Shen, E.D. Honig, R. Kershaw, K. Dwight, and A. Wold, Solid State Ionics 24, 249-252 (1987).
[5] M. Himmrich and H. Haeuseler, Spectrochimica Acta 47A, 933-942 (1991).
[6] J.W. Lekse, M.A. Moreau, K.L. McNerny, J. Yeon, P.S. Halasyamani, and J.A. Aitken, Inorg. Chem. 48, 7516–7518 (2009).
[7] J.W. Lekse, B.M. Leverett, C.H. Lake, and J.A. Aitken, J. Solid State Chem. 181, 3217–3222 (2008).
[8] M.L. Liu, F.Q. Huang, L.D. Chen, and I.W. Chen, Appl. Phys. Lett. 94, 202103/3pp. (2009).
[9] T. Oike and T. Iwasaki, AH01L2915FI, http://www.faqs.org/patents/app/20080303035#ixzz0iW8PX6KV.
[10] S. Nakamura, T. Maeda, and T. Wada, Jpn. J. Appl. Phys. 49, 121203/6pp. (2010).

[11] S. Chen, A. Walsh, Y. Luo, J-H. Yang, X.G. Gong, and S-H. Wei, Phys. Rev. B 82, 195203/8pp. (2010).
[12] G. Gurieva, V. Kravstov, E. Arushanov, S. Schorr, J. Alloys Compd. (submitted).
[13] H-R. Liu, S. Chen, Y-T. Zhai, H.J. Xiang, X.G. Gong, and S-H. Wei, J. Appl. Phys. 112, 093717/6pp. (2012).
[14] S. Levcenco, D. Dumcenco, Y.S. Huang, E. Arushanov, V. Tezlevan, K.K. Tiong, and C.H. Du, J. Alloys Compd.509, 4924–4928 (2011).
[15] S. Levcenco, D. Dumcenco, Y.S. Huang, E. Arushanov, V. Tezlevan, K.K. Tiong, and C.H. Du, J. Alloys Compd.509, 7105–7108 (2011).
[16] S. Levcenco, D.O. Dumcenco, Y.P. Wang, J.D. Wu, Y.S. Huang, E. Arushanov, V. Tezlevan, and K.K. Tiong, Optical Materials 34, 1072–1076 (2012).
[17] N. Mott and E.A. Davies, Electron Processes in Non-Crystalline Materials, Clarendon, Oxford, 1979; N.F. Mott, Metal–Insulator Transitions, Taylor and Francis, London, 1990.
[18] B.I. Shklovskii and A.L. Efros, Electronic Properties of Doped Semiconductors, Springer, Berlin, 1984.
[19] T.G. Castner, Hopping conduction in the critical regime approaching the metal−insulator transition, in: M. Pollak and B. Shklovskii (Eds.), Hopping Transport in Solids, North-Holland, Amsterdam, pp. 1−49, 1991.
[20] M. Guc, K.G. Lisunov, A. Nateprov, S. Levcenko, V. Tezlevan, and E. Arushanov, Mold. J. Phys. Sci. 11, 41–51 (2012).